

Article

# Machine Learning-Based Node Selection for Cooperative Non-Orthogonal Multi-Access System Under Physical Layer Security

Mohammed Ahmed Salem<sup>1</sup>, Azlan Bin Abd.Aziz<sup>1</sup>, Hatem Fahd Al-Selwi<sup>2</sup>, Mohamad Yusoff Bin Alias<sup>3</sup>, Tan Kim Geok<sup>1</sup>, Azwan Mahmud<sup>3</sup>, and Ahmed Salem Bin-Ghooth<sup>1</sup>

<sup>1</sup> Faculty of Engineering and Technology (FET), Multimedia University, Malacca, Malaysia

<sup>2</sup> Faculty of Electrical Engineering (FKE), Universiti Teknikal Malaysia Melaka, Malacca, Malaysia

<sup>3</sup> Faculty of Engineering (FOE), Multimedia University, Selangor, Malaysia

\* Correspondence: mohammedmmu94@gmail.com; Tel.: +60-11-2828-0720

**Abstract:** Cooperative non-orthogonal multi access communication is a promising paradigm for the future wireless networks because of its advantages in terms of energy efficiency, wider coverage, and interference mitigating. In this paper, we study the secrecy performance of a downlink cooperative non-orthogonal multi access (NOMA) communication system under the presence of an eavesdropper node. Smart node selection based on feed forward neural networks (FFNN) is proposed in order to improve the physical layer security (PLS) of a cooperative NOMA network. The selected cooperative relay node is employed to enhance the channel capacity of the legal users, where the selected cooperative jammer is employed to degrade the capacity of the wiretapped channel. Simulations of the secrecy performance metric namely the secrecy capacity ( $C_S$ ) are presented and compared with the conventional technique based on fuzzy logic node selection technique. Based on our simulations and discussions the proposed technique outperforms the existing technique in terms of the secrecy performance.

**Keywords:** Physical layer security (PLS), cooperative relay transmission, non-orthogonal multiple access (NOMA), fuzzy logic, feed forward neural networks (FFNN) secrecy capacity.

## 1. INTRODUCTION

The increasing growth of wireless communication systems has led to eavesdropping attacks. In order to overcome this issue, the enhancement of security in wireless networks becomes an essential factor.

### 1.1. MOTIVATION AND RELATED LITERATURE

The concept of physical layer security (PLS) has been proposed to complement the traditional security solutions such as the cryptographic techniques [1], by exploiting the physical layer properties of the wireless communication network. The baseline of Shannon's cipher system [2] and the developments of Aaron Wyner's Wiretap channel [3] introduce the interests of using the physical wireless characterization to enhance the security of data transmission [4].

Cooperative relay communication is a promising concept for wireless networks due to the advantages of energy efficiency, increasing the coverage and mitigating the interference [5]. The authors of [6] suggest the use of jamming signals generated from the destination node to attack an un-trusted relay that is assumed to be the eavesdropper node. The secrecy performance of this strategy is analyzed in terms of the secrecy outage probability (SOP) metric. The authors of [7] illustrate the benefits and uses of the untrusted relay node in cooperative networks. Moreover, several strategies have been considered in the literature in order to improve the PLS such as cooperative jamming [8]-[9], cognitive radio [10], and energy harvesting [11].

NOMA is an essential enabling technology for the fifth generation (5G) wireless networks to meet the heterogeneous demands on low latency, high reliability, massive connectivity, improved fairness, and high throughput [12]. The key idea behind NOMA is to serve multiple users in the same resource block, such as a

33 time slot, subcarrier, or spreading code. The NOMA principle is a general framework, and several recently  
34 proposed 5G multiple access schemes can be viewed as special cases. In [13], the authors consider the use of  
35 a relay node with two protocols (amplify-and-forward, and decode-and-forward) in a cooperative NOMA  
36 system. The authors of [14] investigate the optimal designs of a NOMA system in terms of the transmission  
37 rates, power allocation for each user, and the decoding factor. In [15], NOMA system is considered in large  
38 scale communication system. In this strategy, the PLS is implemented by using artificial noise generated from  
39 each user node.

40 Smart node selection is an essential and useful strategy in cooperative NOMA communication networks  
41 in terms of enhancing the secrecy performance, saving power and expanding the coverage area. In [16],  
42 the authors consider the combination of cooperative relay and jammer selection based on the buffer-aided  
43 cooperative node selection scheme. The secrecy performance of this strategy is analyzed in terms of SOP  
44 metric. Recently, the integration of cooperative node selection with the artificial intelligence based on fuzzy  
45 logic controller strategy has been proposed to enhance the accuracy of the cooperative node selection strategy.  
46 Motivated by this integration, the authors of [17] propose a relay selection algorithm for a cooperative wireless  
47 sensor networks using fuzzy logic in order to enhance the lifetime and throughput of the network. In [18],  
48 the authors propose a relay selection scheme for multi-user cooperative network, where the cooperative  
49 relay node is selected based on fuzzy logic employed at the base station node. The authors consider four  
50 criteria (SNR, social norm, distance and relays protocol) in the relay selection process based on the channel  
51 state information (CSI) available at the base station. Authors of [19] use a relay selection strategy based on  
52 fuzzy logic with optimal power allocation and adaptive data rate. The authors considered two cases based  
53 on the geographical location of the nodes, where in the first case the distance between the source, relay and  
54 the destination are unknown. However, in the second case each node is assumed to know the geographical  
55 location of the other nodes.

56 Machine learning is a widely growing field in recent modern technologies. This technology has  
57 been integrated with various fields such as, security [20], signal and image processing [21], and wireless  
58 communication networks [22]. In security, machine learning techniques such as neural networks have  
59 been investigated and illustrated in considerable researches. In [23], the authors use the artificial neural  
60 networks (ANNs) technique as a relay selection method in a detect-and-forward multi-relaying network. The  
61 aim of using this method is to enhance the physical layer security of the network. Thus, the transmission  
62 between a source and a destination is secure in the presence of an eavesdropper node. Authors of [24] exploit  
63 two machine learning based physical layer security techniques namely, Naïve Bayes (NB) and support  
64 vector machine (SVM). The authors investigate the benefits of machine learning approach in order to  
65 improve the physical layer security in the presence of MIMO-Multi-antenna eavesdropper nodes. In wireless  
66 communication networks, machine learning approach has been used in several researches such as channel  
67 estimation [25], power allocation [26], and best antenna selection [27].

68 Based on [17], the network lifetime and end-to-end throughput is enhanced by using node selection  
69 based on artificial intelligence strategies. To the best of the authors' knowledge, applying the smart node  
70 selection based on neural network methods in cooperative NOMA system under the physical layer security  
71 has not been adequately investigated in the literature. In this paper, the smart node selection based on feed  
72 forward neural networks integrated with the null-steering jamming strategy in a cooperative NOMA network  
73 is analysed to select the best cooperative relay or jammer nodes in the presence of an eavesdropper node.

## 74 1.2. MAIN CONTRIBUTIONS

75 Unlike the summarized papers above, this paper investigates the secrecy capacity of a cooperative  
76 NOMA communication network integrated with a smart node selection strategy based on feed forward neural  
77 networks. The main contributions of this paper are summarized as follows.

- 78 • We integrate the use of jammer and relay nodes to degrade the capacity of the eavesdropper node and  
79 enhance the capacity of the user node respectively. We use the null-steering beamforming technique to  
80 direct the shared jamming signal towards the eavesdropper node.

- 81 • We employ the feed forward neural network (FFNN) strategy in order to select the best cooperative node  
 82 for the relaying or jamming techniques. This approach is compared with another selection approach  
 83 based on fuzzy logic strategy.

84 The rest of this paper is organized as follows. Section 2 demonstrates the system model and the signal  
 85 transmission. Section 3 presents the node selection strategies. Section 4 explains the secrecy performance  
 86 analysis of the system model. Section 5 shows the results and discussions of the paper. Finally, section 6  
 87 presents the conclusion of this paper.

## 88 2. SYSTEM MODEL

89 We consider a secure non-orthogonal multi access (NOMA) system, where a base station ( $B_s$ )  
 90 communicates with a strong user ( $User_1$ ) (good channel conditions) and a weak user ( $User_2$ ) (poor channel  
 91 conditions) in the presence of a passive eavesdropper node which is able to monitor the main channel,  
 92 as shown in Figure 1. The cooperative helper nodes ( $R_1, R_2, \dots, R_N$ ) are employed to enhance the secrecy  
 93 performance of the communication scenario. In this system model, the users and the eavesdropper nodes  
 94 are equipped with a single antenna. However, the helper nodes are equipped with  $M$  antennas. Moreover, the  
 95 transmission time is divided to time frames in which each time frame is divided into two time slots (phases).

96 In this system model, we assumed that the eavesdropper node is a passive communication node which  
 97 has no access to the information signal transmitted to the receiver node. Moreover, we assumed that the  
 98 eavesdropper node has the ability of differentiating and detecting the superimposed data transmitted from  
 99 the base station to the users [28]. This assumption provides the lower bounds for the practical scenario, where  
 100 the eavesdropper node is given a strong decoding capabilities.

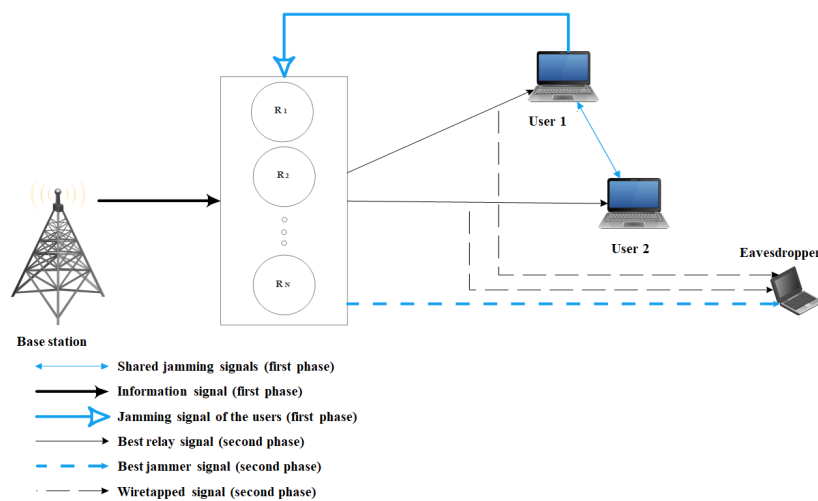


Figure 1. System model

### 101 2.1. COOPERATIVE HELPER (RELAY AND JAMMER) NODES

102 Cooperative communication techniques are employed either to strengthening the legal main channel  
 103 of the user nodes (by using cooperative relay nodes) or to degrade the illegal wiretapped channel of the  
 104 eavesdropper node (by using cooperative jammer node) [29]-[30]. The use of these techniques enhances  
 105 significantly the secrecy performance of the NOMA system. In this paper, we used both techniques in order  
 106 to have a secure communication between the base station and the user nodes. Moreover, the eavesdropper's  
 107 channel state information (CSI) is assumed to be available at the base station and the cooperative helper  
 108 nodes [32]. The cooperative helper node is selected as a cooperative relay node or a cooperative jammer by  
 109 using a node selection method based on fuzzy logic and feed forward neural networks strategies.

110 In this paper, the relay is assumed to be a half-duplex two-way with an amplify-and-forward protocol.  
 111 The relay is used as transmission node between the base station and the users with no direct channel between

base station and users. Thus, the communication happens in two time slots (phases) as illustrated in Figure 1. Moreover, the cooperative relay node is used in order to enhance and improve the channel capacity of the user nodes.

In this work, the cooperative jammer node uses the CSI information to build a jamming-null-steering beamforming strategy, where the shared jamming signals generated by the users are directed to the eavesdropper node. However, the shared jamming signals are nulled in the directions of the legal user nodes. This strategy ensures that the communication channel between the friendly jammer and the legal user nodes is not available. Thus, the channel capacity of the eavesdropper node is degraded without affecting the legal user nodes. The jamming-null-steering beamforming at the jammer node is expressed as,

$$NB_E = \frac{(I_M - W) h_{R_j,E}}{\|(I_M - W) h_{R_j,E}\|} \quad (1)$$

where,  $I_M$  is the identity matrix with  $M * M$ ,  $W$  is the projection matrix to the orthogonal subspace of the legal user nodes with  $W = G(G^H G)^{-1} G^H$ ,  $G = [h_{R_j,U_1} h_{R_j,U_2}]$ , and  $h_{R_j,U_1}$ ,  $h_{R_j,U_2}$  and  $h_{R_j,E}$  are the channel gains between the friendly jammer node and the legal user nodes ( $U_1, U_2$ ) and the eavesdropper node respectively.

## 2.2. CHANNEL ASSUMPTIONS

In this model, the communication links between the nodes are assumed to be Rayleigh fading channel with exponential path loss. The coefficient of a channel link between two nodes is expressed by  $h_{ab}$ , where  $a$  is the node where the transmission starts and,  $b$  is the node where the transmission ends. These coefficients are modelled as constant and identically distributed at the transmission phases. Moreover, the channel state information (CSI) of the users and the eavesdropper nodes are assumed to be perfectly available at the base station and the cooperative helper nodes. However, In practice, the user nodes estimate the absolute values of the CSI from the cooperative nodes to the eavesdropper node then feed it back to the base station via the cooperative nodes. Furthermore, the noise is assumed to be a complex additive white Gaussian noise (AWGN) with zero mean and unit variance.

## 2.3. SIGNAL TRANSMISSION MODEL

This section explains the flow of the transmitted superimposed information signal from the base station to the user nodes via the cooperative relay node and under the protection of the cooperative jammer node.

In the first phase, the base station transmits the superimposed information signals to the helper nodes. The received signal at each helper node is written as,

$$X_{BS,R_i} = \sqrt{P_{BS} a_{u_1}} h_{BS,R_i} B_{U_1} x_1 + \sqrt{P_{BS} a_{u_2}} h_{BS,R_i} B_{U_2} x_2 + n_{BS,R_i} \quad (2)$$

where,  $P_{BS}$  is the power of the base station,  $a_{u_1}$  and  $a_{u_2}$  are the power allocation coefficient for  $user_1$  and  $user_2$  respectively,  $x_1$  and  $x_2$  are the information to  $user_1$  and  $user_2$  respectively,  $h_{BS,R_i}$  is the channel gain between the base station and the helper node, the subscript  $i$  stands for the number of the cooperative helper node,  $B_{U_1}$ ,  $B_{U_2}$  are the maximum ratio transmission beamforming vector build by the base station for the strong user and the weak user respectively, and  $n_{BS,R_i}$  is the AWGN noise from the base station to the helper node. At the same phase,  $user_1$  and  $user_2$  generate jamming signals and share these signals. The shared jamming signals are given as,

$$J_{u_1} = \sqrt{P_{u_1}} h_{u_1,u_2} j_1 + n_{u_1,u_2}$$

$$J_{u_2} = \sqrt{P_{u_2}} h_{u_2,u_1} j_2 + n_{u_2,u_1} \quad (3)$$

where,  $P_{u_1}$  and  $P_{u_2}$  are the powers of the users respectively,  $j_1$  and  $j_2$  are the artificial jamming signals from  $user_1$  and  $user_2$  respectively,  $h_{u_1,u_2}$  and  $h_{u_2,u_1}$  are the channel gains between the users, and  $n_{u_1,u_2}$  and

149  $n_{u_2, u_1}$  are the AWGN noise between the users. The shared jamming signals are transmitted by the strong user  
 150 to the helper nodes. The received jamming signal at each helper node is given as,

$$J_{u_1, R_i} = (J_{u_1} + J_{u_2}) h_{u_1, R_i} + n_{u_1, R_i} \quad (4)$$

151 where,  $h_{u_1, R_i}$  is the channel gain between the strong user and the helper node and  $n_{u_1, R_i}$  is the AWGN  
 152 noise from the strong user to the helper node.

153 At this stage each helper node is aware of the received signals from the legitimate nodes. These signals  
 154 are summarised as follows.

- 155 • The superimposed information signal transmitted by the base station. Equation 2 illustrates the  
 156 superimposed information signal received at the helper nodes.
- 157 • The shared jamming signal transmitted by strong user. Equations 3 and 4 demonstrate the shared  
 158 jamming signal received at the helper nodes.

159 In the second phase, the selected cooperative relay node amplifies-and-forwards the superimposed  
 160 information signal to the user nodes. The amplification factor ( $A_F$ ) is expressed as [33],

$$A_F = \sqrt{\frac{P_{R_s}}{P_{BS} |h_{BS, R_s}|^2 + P_{u_1} |h_{u_1, R_i}|^2 + \sigma}} \quad (5)$$

161 where,  $P_{R_s}$  is the power of the selected cooperative relay node, the subscript  $s$  stands for the selected  
 162 cooperative relay node, and  $\sigma$  denotes the variance of the AWGN noise.

163 The forwarded signal to the strong user ( $user_1$ ) is expressed as,

$$Y_{R_s, u_1}^{A_F} = [A_F h_{R_s, u_1} (X_{BS, R_s})] + n_{R_s, u_1} \quad (6)$$

164 The forwarded signal to the weak user ( $user_2$ ) is expressed as,

$$Y_{R_s, u_2}^{A_F} = [A_F h_{R_s, u_2} (X_{BS, R_s})] + n_{R_s, u_2} \quad (7)$$

165 At the same phase, the eavesdropper wiretaps the main channel in order to receive the transmitted  
 166 signal from the cooperative relay to the user nodes. However, the selected cooperative jammer node directs  
 167 the shared jamming signal towards the eavesdropper node. The received signal at the eavesdropper node  
 168 under the protection of the selected cooperative jammer node is given as,

$$Y_{R_s, E}^{A_F} = A_F h_{R_s, E} X_{BS, R_s} + h_{R_j, E} J_{u_1, R_j} NB_E + n_{R_s, E} \quad (8)$$

169 where,  $NB_E$  is the jamming-null-steering beamforming vector build by the selected cooperative jammer  
 170 node,  $h_{R_j, E}$  is the channel gain between the selected cooperative jammer node and the eavesdropper node,  
 171 and the subscript  $j$  stands for selected cooperative jammer node.

### 172 3. SMART NODE SELECTION STRATEGIES

173 In this section, we illustrate the cooperative node selection based on fuzzy logic (FL) and feed forward  
 174 neural network (FFNN) strategies.

#### 175 3.1. FUZZY LOGIC SELECTION

176 Figure 2 demonstrates the general flowchart of the fuzzy logic strategy used to select the best cooperative  
 177 relay and jammer node respectively.

178 Based on Figure 2, three main steps are required to select the best cooperative relay or jammer nodes  
 179 based on the fuzzy logic controller strategy.

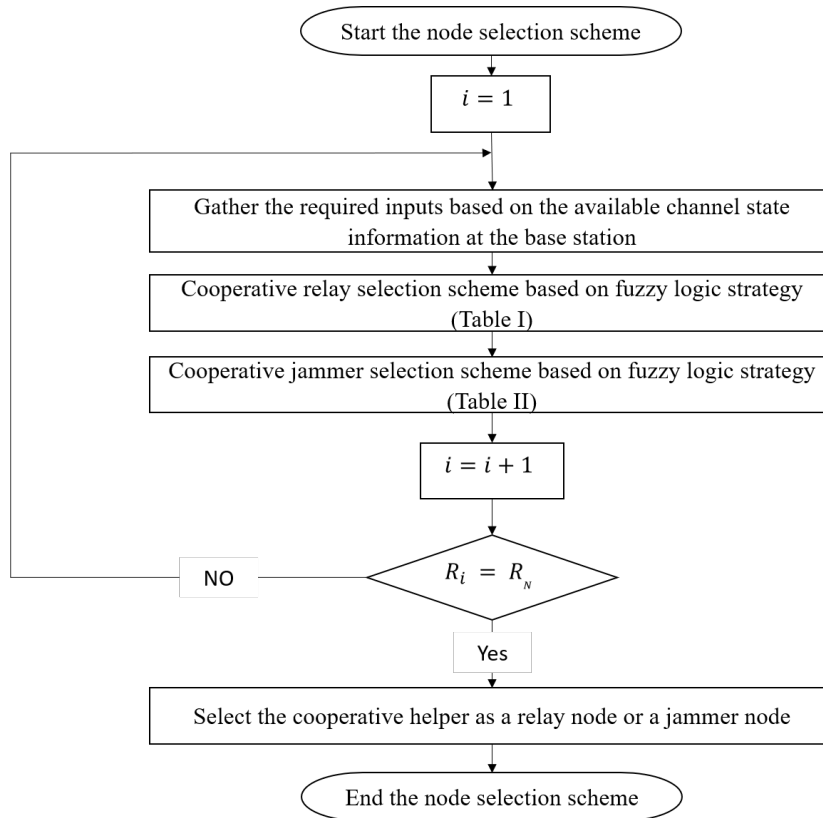


**Figure 2.** Flowchart of cooperative node selection based on fuzzy logic

### 180 3.1.1. Required input gathering

181 At the end of each time frame the base station gathers the estimated information of network users, and  
 182 at the beginning of each time frame the base station selects the best cooperative relay enhance the legal  
 183 channel capacity and the best cooperative jammer to degrade the wiretapped channel capacity. To this end,  
 184 the base station should estimate five parameters namely, signal to noise ratio for the legal users ( $SNR_U$ ),  
 185 power amplification factor ( $PAF$ ), the distance between the cooperative helper and legal user nodes ( $D_U$ ),  
 186 signal to noise ratio for the eavesdropper ( $SNR_E$ ), and the distance between the cooperative helper and the  
 187 eavesdropper ( $D_E$ ). These parameters are gathered with the help of the channel state information (CSI)  
 188 available at the base station. In order to use these parameters in the fuzzy logic model, we normalized the  
 189 each parameter value to the interval  $[0,1]$ .

- 190 • Signal to noise ratio (for the legal users  $SNR_U$ )

191 Signal-to-noise ratio is the main criterion in the process of helper selection. The SNR values for the  
 192 system model shown in Fig 1 are calculated as,

$$\xi_{u_1} = \frac{A_F^2 P_{BS} a_{u_1} |h_{R_i, u_1}|^2 |h_{BS, R_i}|^2}{(A_F^2 |h_{R_i, u_1}|^2 + 1) \sigma^2} \quad (9)$$

$$\xi_{u_2} = \frac{A_F^2 P_{BS} a_{u_2} |h_{R_i, u_2}|^2 |h_{BS, R_i}|^2}{A_F^2 P_{BS} a_{u_1} |h_{R_i, u_2}|^2 |h_{BS, R_i}|^2 + (A_F^2 |h_{R_i, u_2}|^2 + 1) \sigma^2} \quad (10)$$

193 We mapped the maximum normalized  $SNR_U$  into low, medium and high as shown in Figure 3 (a). The  
 194 maximum SNR is chosen as,

$$SNR_U = \max\{\xi_{u_1}, \xi_{u_2}\} \quad (11)$$

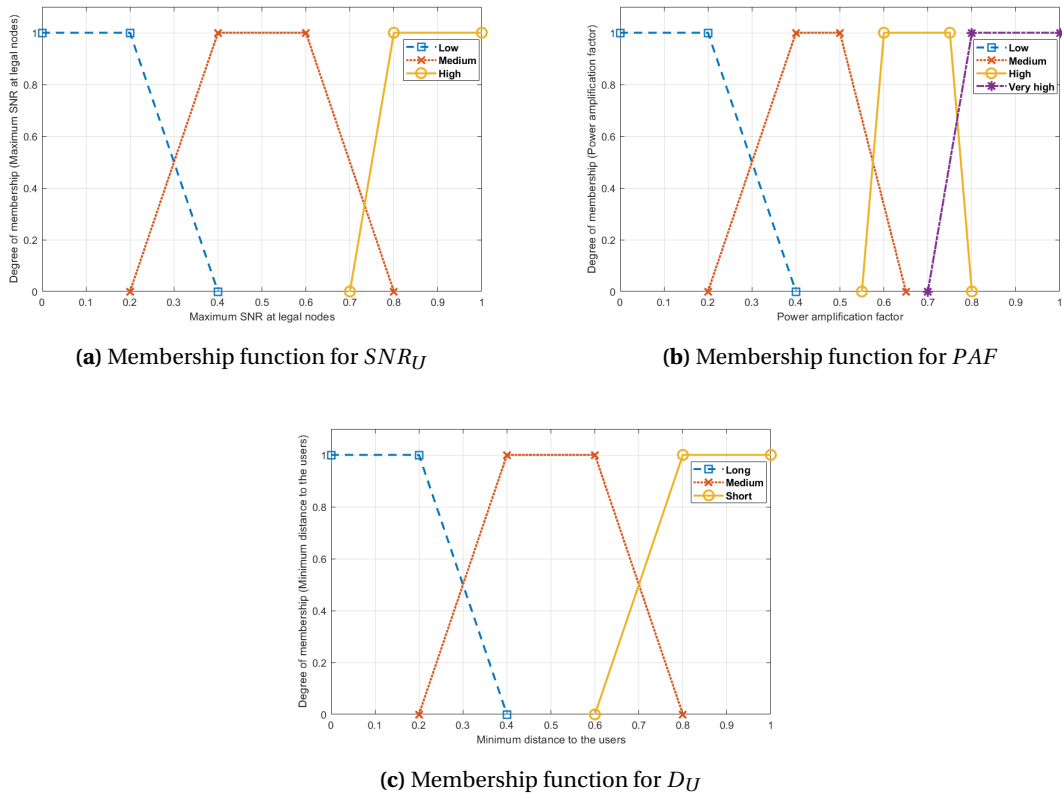


**Figure 3.** Membership function for cooperative relay input fuzzy sets

- 195 • Power amplification factor ( $PAF$ )

196 Power amplification factor is a direct aspect to enhance the capacity of the main communication  
 197 channels between the selected cooperative relay node and the legal user nodes. Equation (5) is used in order  
 198 to calculate the power amplification factor. We mapped the normalized power amplification factor into low,  
 199 medium, high and very high as shown in Figure 3 (b).

- 200 • Distance between the cooperative helper and legal user nodes ( $D_U$ )

201 The helper location has significant impact on average achievable rate at the receiver nodes. The distances  
 202 between the helper nodes and the legal user nodes are calculated as,

$$D_{U_1} = \sqrt{(X_{U_1} - X_{R_i})^2 + (Y_{U_1} - Y_{R_i})^2}$$

$$D_{U_2} = \sqrt{(X_{U_2} - X_{R_i})^2 + (Y_{U_2} - Y_{R_i})^2}$$
(12)

203 where,  $X_{U_1}$ ,  $X_{U_2}$  and  $X_{R_i}$  are the coordinates of the horizontal axis for  $user_1$ ,  $user_2$  and the cooperative  
 204 helper node  $i$ , and  $Y_{U_1}$ ,  $Y_{U_2}$  and  $Y_{R_i}$  are the coordinates of the vertical axis for  $user_1$ ,  $user_2$  and the cooperative  
 205 helper node  $i$ . In this work, we choose the minimum distance between the cooperative helper and legal  
 206 nodes. The minimum distance is given as,

$$D_U = \min \{D_{U_1}, D_{U_2}\}$$
(13)

207 We mapped the normalized minimum distance ( $D_U$ ) into long, medium and short as shown in Figure 3  
 208 (c).

- 209 • Signal to noise ratio (for the eavesdropper  $SNR_E$ )

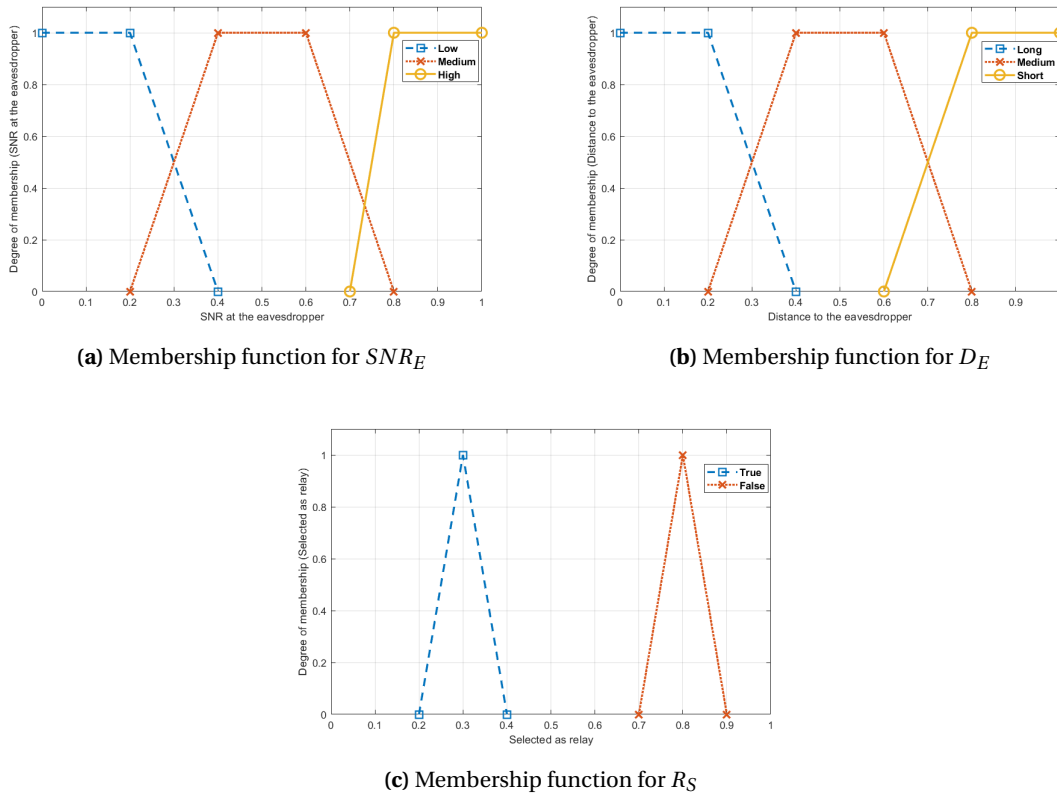


**Figure 4.** Membership function for cooperative jammer input fuzzy sets

210 The SNR values for the eavesdropper node is expressed as,

$$\xi_E = \frac{A_F^2 P_{BS} a_m |h_{R_i,E}|^2 |h_{BS,R_i}|^2}{A_F^2 |h_{R_i,E}|^2 J_{u_1,R_i} |NB_E|^2 + (A_F^2 |h_{R_i,E}|^2 + 1) \sigma^2} \quad (14)$$

211 where,  $m \in (U_1, U_2)$ . We mapped the normalized  $SNR_E$  into low, medium and high as shown in Figure 4  
212 (a).

- 213 • Distance between the cooperative helper and the eavesdropper ( $D_E$ )

214 The distances between the helper nodes and the eavesdropper node are calculated as,

$$D_E = \sqrt{(X_E - X_{R_i})^2 + (Y_E - Y_{R_i})^2} \quad (15)$$

215 We mapped the normalized distance ( $D_E$ ) into long, medium and short as shown in Figure 4 (b).

- 216 • The cooperative helper node is selected as the best relay ( $R_S$ )

217 In this work, the priority is given to the relay selection. In other words, the output for the degree of relay  
218 node relevance is fed as an input for the jammer node selection. Hence, if the cooperative helper node is  
219 selected as a relay then the degree of jammer relevance for that node is very bad. We mapped the relay node  
220 selection into true and false as shown in Figure 4 (c).

221 This step is summarized as follows.

- 222 • The required parameters are gathered based on the available channel state information (CSI) at the  
223 base station node.
- 224 • Each parameter is mapped in a fuzzy set. the fuzzy sets are as follows.



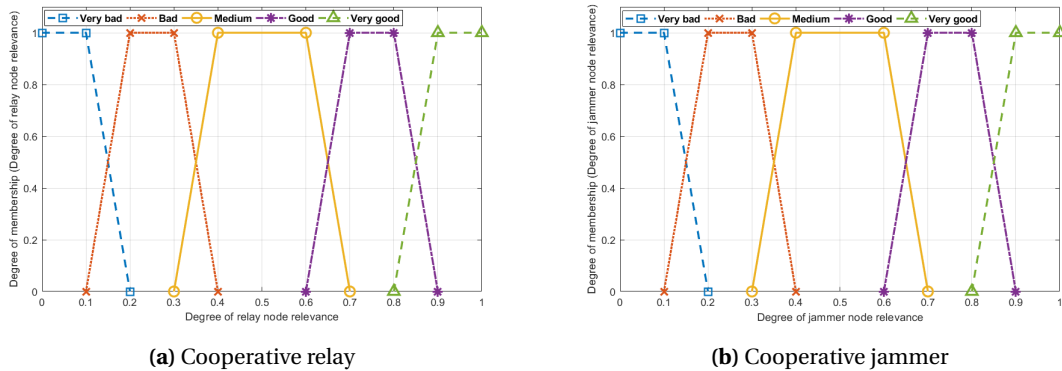


Figure 5. Membership function for degree of cooperative node relevance

- 225       –  $SNR_U \in \{ \text{Low, Medium, High} \}$   
 226       –  $PAF \in \{ \text{Low, Medium, High, Very high} \}$   
 227       –  $D_U \in \{ \text{Long, Medium, Short} \}$   
 228       –  $SNR_E \in \{ \text{Low, Medium, High} \}$   
 229       –  $D_E \in \{ \text{Long, Medium, Short} \}$   
 230       –  $R_S \in \{ \text{True, False} \}$

### 231 3.1.2. Process of Fuzzification

232       In this step, we use the fuzzy inference system (FIS) to obtain the fuzzy sets  $Z_r$  and  $Z_j$  that maps  
 233       the degree of relevance for relay and jammer respectively. However, these fuzzy sets are a description of  
 234        $f_r(SNR_U, PAF, D_U)$  and  $f_j(SNR_E, D_U, R_S)$  functions. The relevance fuzzy sets are given as.

$$\begin{aligned} Z_r &\in \{ \text{Very bad, Bad, Medium, Good, Very good} \} \\ Z_j &\in \{ \text{Very bad, Bad, Medium, Good, Very good} \} \end{aligned} \quad (16)$$

235       where, very bad, bad, medium, good, and very good are the degree of relevance for each cooperative  
 236       node. In other word, if the degree of relaying relevance for any cooperative node is very good, then the  
 237       probability of selecting this node as a relay is high. Figure 5 shows the membership function for the relay  
 238       and jammer nodes relevance fuzzy sets respectively. In this work, we use AND logic in determining the fuzzy  
 239       rules and in order to map the input fuzzy sets  $(SNR_U, PAF, D_U, SNR_E, D_U, R_S)$  into the relevance fuzzy sets  
 240        $(Z_r, Z_j)$ . Table 1 summarizes the fuzzy rules for the cooperative relay selection scheme.

Table 1. Rules for relay selection scheme

SNR	Distance	Power amplification factor			
		Low	Medium	High	Very High
Low	long	Very bad	Bad	Bad	Medium
Low	Medium	Very bad	Bad	Bad	Medium
Low	Short	Very bad	Medium	Medium	Medium
Medium	long	Very bad	Medium	Medium	Medium
Medium	Medium	Bad	Medium	Good	Good
Medium	Short	Bad	Medium	Good	Good
High	long	Bad	Medium	Medium	Good
High	Medium	Medium	Good	Good	Very Good
High	Short	Medium	Good	Very Good	Very Good

241       In this paper, we have 36 fuzzy rules for the cooperative relay selection scheme and 18 fuzzy rules for the  
 242       cooperative jammer selection scheme. Note that the priority is for the cooperative relay selection scheme, so

243 the cooperative relay node is selected first, then the cooperative jammer node is selected. Table 2 summarizes  
244 the fuzzy rules for the cooperative jammer selection scheme.

**Table 2.** Rules for jammer selection scheme

SNR	Distance	The node is selected as relay	
		True	False
Low	long	Very bad	Medium
Low	Medium	Very bad	Good
Low	Short	Very bad	Very good
Medium	long	Very bad	Bad
Medium	Medium	Very bad	Medium
Medium	Short	Very bad	Medium
High	long	Very bad	Very bad
High	Medium	Very bad	Bad
High	Short	Very bad	Bad

### 245 3.1.3. Process of defuzzification

246 This section illustrates the process of obtaining the output (degree of (relay or jammer) relevance). In  
247 order to obtain the outputs of the fuzzy logic system we used the process of crisp output center of sum  
248 defuzzification method denoted as  $z_{crisp}$ . Firstly, the fuzzy logic controller calculates the geometric centre of  
249 area defined as COA for all the membership function of the relay and jammer degree of relevance [34]. The  
250 geometric centre of area is given as,

$$COA_{Z_r} = \frac{\int \mu_{Z_r}(Z_r) Z_r dZ_r}{\int \mu_{Z_r}(Z_r) dZ_r}$$

$$COA_{Z_j} = \frac{\int \mu_{Z_j}(Z_j) Z_j dZ_j}{\int \mu_{Z_j}(Z_j) dZ_j} \quad (17)$$

251 Finally, the controller calculates weighted average for the geometric centre of area for all the membership  
252 function of the relay and jammer degree of relevance. The weighted average for the geometric centre of area  
253 is given as,

$$z_{crisp_r} = \frac{\sum_{i=1}^N COA_{z_{r_i}} \cdot A_{z_{r_i}}}{\sum_{i=1}^N A_{z_{r_i}}}$$

$$z_{crisp_j} = \frac{\sum_{i=1}^N COA_{z_{j_i}} \cdot A_{z_{j_i}}}{\sum_{i=1}^N A_{z_{j_i}}} \quad (18)$$

254 where,  $A$  is the area under the scaled membership functions for the relay ( $A_{z_{r_i}}$ ) and jammer ( $A_{z_{j_i}}$ ) degree  
255 of relevance and within the range of the output variable.

## 256 3.2. MACHINE LEARNING-BASED FEED FORWARD NEURAL NETWORK SELECTION

257 In this paper, a machine learning FFNN-based algorithm is proposed in order to select the best  
258 cooperative relay and jammer nodes respectively. In this section, the main steps for the proposed strategy are  
259 explained in detail.

### 260 3.2.1. Input Data Generation

261 For training the FFNN model, cooperative relay and jammer data are generated containing  $L$  samples.  
262 The generated data is extracted from the known CSI at the base-station node. The generated relay data  
263 denoted as  $GD_R$  consists of three parameters, namely  $SNR_U$ ,  $PAF$ , and  $D_U$ . Similarly, the generated jammer

264 data denoted as  $GD_J$  consist of three parameters, namely  $SNR_E$ ,  $D_E$ , and  $R_S$ . These parameters are expressed  
 265 as,

$$GD_R = [SNR_U, PAF, D_U]^L \quad (19)$$

$$GD_J = [SNR_E, R_S, D_E]^L \quad (20)$$

266 where,  $SNR_U, PAF, D_U, SNR_E, R_S$  and  $D_E$  are the estimated information of the network users gathered  
 267 by the base-station at the end of each frame. We normalized the generated data to the interval  $[0,1]$ .

### 268 3.2.2. Output Labelling

269 In the data generated, the degree of relay node relevance and the degree of jammer relevance are chosen  
 270 as the performance indicators for relay and jammer respectively. Each training data sample is associated with  
 271 a performance indicator corresponding to the current sample. Table 3 illustrates the labelling of cooperative  
 272 nodes relevance.

**Table 3.** Labelling the relevance of the cooperative nodes

Cooperative (relay or jammer) relevance	Label (t)
Very bad	0
Bad	1
Medium	2
Good	3
Very good	4

273 Based on Table 3, the training data samples are labelled according to the performance of each relay and  
 274 jammer nodes respectively.

### 275 3.2.3. Data Set Training

276 After generating the input samples and output labels, the input-output pairs are concatenated to create  
 277 two full data sets for relay and jammer respectively.

$$D_{relay\ train} = \{([GD_R]^1, t^1), ([GD_R]^2, t^2), \dots, ([GD_R]^L, t^L)\} \quad (21)$$

$$D_{jammer\ train} = \{([GD_J]^1, t^1), ([GD_J]^2, t^2), \dots, ([GD_J]^L, t^L)\} \quad (22)$$

278 where,  $t^L$  is the Lth class label.

### 279 3.2.4. FFNN structure

280 The labelled training data sets is used to train the FFNN model. The input of the models are absolute  
 281 values of the generated data ( $GD_R, GD_J$ ) and the output is the performance of the relay or jammer. The  
 282 output of the model indicates the degree of relevance for relay and jammer respectively. Here, the basics of  
 283 the neural network is described briefly. The structure of the FFNN model consists of multiple hidden layers,  
 284 each hidden layer contains multiple neutral nodes. After each layer a nonlinear function (activation function)  
 285 is implemented. Due to their efficiency in generalizing the trained model, the nonlinear activation functions  
 286 are the most used activation functions, the most common choices of these functions is the rectified linear  
 287 unit (*ReLU*) function expressed by,

$$f_{ReLU}(x) = \max(0, x) \quad (23)$$

288 where,  $x$  is the argument of the function. Choosing an activation function is a vital step when building  
 289 a neural network model and ensures a good performance model. In this experiment, the ReLU function is  
 290 applied to all hidden layers where it enables the model to learn more complex structures and generalize to  
 291 variety of data. Our experiment is a multi-class classification case. Thus, an activation function is used at the  
 292 output layer expressed by,

$$f_{Softmax}(x_i) = \frac{\exp(x_i)}{\sum_{j=1}^C \exp(x_j)} \quad (24)$$

293 where,  $C$  is the number of classes,  $i, j \in 1, 2, \dots, C$ , and  $x_i, x_j$  are scores of the  $i$ th class and  $j$ th class,  
 294 respectively. The network model consists of four layers namely, input, two hidden and output layers. The  
 295 input layer takes input parameters ( $GD_R, GD_J$ ) for relay or jammer nodes receptively. Figure 6 shows the  
 296 feed forward neural networks design model.

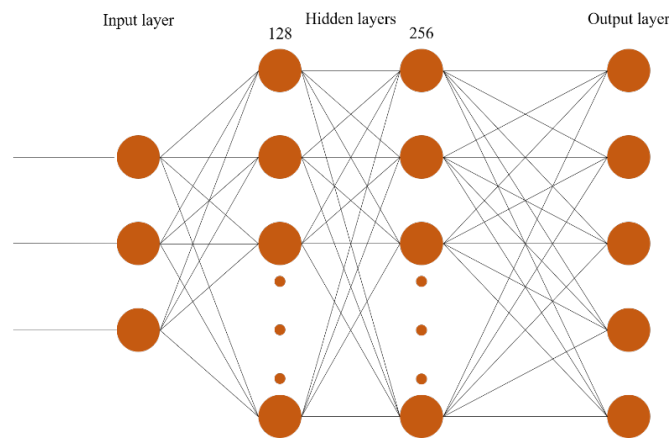


Figure 6. FFNN design model

297 Based on Figure 6, the first and the second hidden layers consist of 128, 256 neurons, respectively.  
 298 The output layer consists of five neurons corresponding to the classes of the cooperative (relay or jammer)  
 299 relevance. Softmax function is applied to this layer which gives us the probability distribution over all classes.  
 300 The final output of the network is the class with the maximum probability value.

### 301 3.2.5. FFNN training

302 In this section, the process of setting the training parameters of our FFNN model is described. In total,  
 303 two data sets were generated using two groups of data samples, 60000 samples of relay data ( $GD_R$ ) and  
 304 60000 samples of jammer data ( $GD_J$ ). Two models were trained using the two data sets of relay and jammer  
 305 respectively. The training data sets were split into the training set and the testing set. The training set was  
 306 used to train the model parameters and the testing set was used to evaluate the trained model. In this FFNN  
 307 model, cross entropy is applied as the loss function for our FFNN model. Therefore, the loss function for each  
 308  $i$ th sample of input  $GD_R$  of relay data and each  $j$ th sample of input  $GD_J$  of jammer data is formulated as,

$$\begin{aligned} Loss_R(t^i, o(GD_R^i, W, b)) &= -\log(o(GD_R^i, W, b)) \\ Loss_J(t^j, o(GD_J^j, W, b)) &= -\log(o(GD_J^j, W, b)) \end{aligned} \quad (25)$$

309 where,  $o(GD_R^i, W, b)$  is the output that is predicted by the model for the best cooperative relay node.  
 310 The target of the training process is to find the suitable parameters  $W$  and  $b$  that minimize the average loss  
 311 "cost function" of entry training data sets, the cost function is defined as,

$$L_R(\Theta) = \frac{1}{M} \sum_{i=1}^M Loss(t^i, o(GD_R^i, W, b))$$

$$L_J(\Theta) = \frac{1}{M} \sum_{j=1}^M \text{Loss}(t^j, o(GD_J^j, W, b)) \quad (26)$$

where the set  $\Theta = \{W, b\}$  contains every training parameter of the FFNN model. Every parameter is generally adjusted iteratively using the gradient descent methods. At each iteration, every parameter is adjusted simultaneously as,

$$\Theta^{m+1} = \Theta^m - \eta \nabla_{\Theta} L(\Theta), \quad (27)$$

where  $\nabla_{\Theta}$  represents as the gradient operator with respect to  $\Theta$ ,  $\eta$  is the learning rate, and  $m$  is the iteration number (250 iterations). Backpropagation is used to update the weights  $W$  and biases  $b$  of the neural network using the local error of the network. During training the network, when a prediction is made for the input values, the actual output values are compared to the predicted values and an error is calculated. The calculated error is then used to update the weights  $W$  and biases  $b$  of the network starting at the layers connected directly to the output nodes and then proceeding further backward toward the binput layer. In other words, the backpropagation is used to calculate the gradients efficiently which is then used to train the network, by adjusting the weights  $W$  and biases  $b$  throughout the network to get the desired output.

In this experiment, Adam optimization algorithm was applied to the FFNN model because it is a first-order gradient-based optimization algorithm, thus reducing computational complexity [17]. In addition, the dropout technique is applied in this FFNN model in order to reduce the overfit in training and improve generalization of the model (0.5 dropout was chosen), for which the proposed FFNN model performs well. Finally, after training and testing the two models of relay and jammer respectively, the FFNN models are frozen and can be used to select the best cooperative helper node as a relay or jammer.

#### 4. SECRECY PERFORMANCE ANALYSIS

In this section, we illustrate the secrecy performance metric in terms of the secrecy capacity for the system model shown in Figure 1 assisted with the fuzzy logic and the feed forward neural network strategies. The secrecy capacity metric is defined as the maximum capacity rate difference between the channel capacity of the legitimate users and the channel capacity of the eavesdropper node. The channel capacity of the strong user ( $user_1$ ) is given as,

$$\zeta_{u_1} = \frac{1}{2} \log_2(1 + \xi_{u_1}) \quad (28)$$

where,  $\xi_{u_1}$  is the signal to noise ratio (SNR) at the strong user expressed in equation (9). The strong user is able to decode the weak user's information signal and suppressed it by using the successive interference cancellation (SIC) strategy. The channel capacity of the weak user ( $user_2$ ) is given as,

$$\zeta_{u_2} = \frac{1}{2} \log_2(1 + \xi_{u_2}) \quad (29)$$

where,  $\xi_{u_2}$  is the signal to interference plus noise ratio (SINR) at the weak user expressed in equation (10). The weak user is not able to decode the strong user's information signal, so the strong user's information signal is an interference to the weak user. The channel capacity of the eavesdropper node is given as,

$$\zeta_E = \frac{1}{2} \log_2(1 + \xi_E) \quad (30)$$

where,  $\xi_E$  is the signal to jamming plus noise ratio (SJNR) at the eavesdropper node expressed in equation (14). We assume that the eavesdropper node is able to distinguish the superimposed mixture signal by using the parallel interference cancellation (PIC) strategy. The secrecy capacity for each user is formulated as,

$$[\zeta_{u_1}^E]^+ = \max\{\zeta_{u_1} - \zeta_E, 0\}$$

$$[\zeta_{u_2}^E]^+ = \max\{\{\zeta_{u_2} - \zeta_E\}, 0\} \quad (31)$$

344 In order to evaluate the accuracy of the proposed cooperative node selection strategy, the error analysis  
 345 is carried on by comparing the secrecy capacity achieved based on the fuzzy logic and the FFNN strategies  
 346 with maximum secrecy capacity of the system model.

347 In this paper, the maximum secrecy capacity is achieved when the eavesdropper node does not exist.  
 348 The maximum secrecy capacity at each user is respectively formulated as,

$$[\zeta_{u_1}^{max}]^+ = \max\{\{\zeta_{u_1}\}, 0\}$$

$$[\zeta_{u_2}^{max}]^+ = \max\{\{\zeta_{u_2}\}, 0\} \quad (32)$$

349 In this section, the accuracy percentage ( $A_p$ ), and the root mean square error ( $RMSe$ ) equations for  
 350 both users are respectively given as,

$$A_{p_{u_m}} = \left( 1 - \left| \frac{[\zeta_{u_1}^{max}]^+ - [\zeta_{u_m}^E]^+}{[\zeta_{u_m}^{max}]^+} \right| \right) \times 100\% \quad (33)$$

$$RMSe_{u_m} = \sqrt{\frac{\sum_{k=1}^K \left( [\zeta_{u_m}^{max}]^+ - [\zeta_{u_m}^E]^+ \right)^2}{K}} \quad (34)$$

351 where,  $K$  is the maximum repetition based on the maximum transmit power.

## 352 5. RESULTS AND DISCUSSION

353 In this section, the numerical results are obtained and discussed to evaluate the secrecy performance of  
 354 the proposed cooperative NOMA assisted with null-steering beamforming jamming and node selection based  
 355 on FFNN technique. The simulation setup parameters of the proposed technique are summarized in Table 4.

**Table 4.** SIMULATION SET UP PARAMETERS

PARAMETER	DETAILS
Cooperative nodes	Five cooperative nodes
Nodes locations	Illustrated in Figure 7
Power allocation for the strong user	0.2
Power allocation for the weak user	0.8
Total transmission power	30 dBm
Path loss coefficient	3.5
Noise density	-60 dBm
Channel model	Slow fading Rayleigh channel
Defuzzification process	Crisp output center of sum

356 Figure 7 shows the geographical locations of the cooperative NOMA system for all the nodes. These  
 357 locations are used in order to simulate the experiments (1 and 2).

358 Table 4 and Figure 7 illustrate that five cooperative helper nodes are used in order to complete the  
 359 relaying and jamming processes. However, the data relaying process is done by a single cooperative relay node  
 360 selected by using a smart node selection strategy discussed in section 4. Similarly, jamming the eavesdropper  
 361 node is done by a selected cooperative jammer node.

362 The distances between the base station and the cooperative helper nodes are assumed to be  
 363 non-equidistant to the distances between the relay nodes and the legal users. The eavesdropper is positioned  
 364 at a fixed coordinates (1500, -200) about 1513.28 meters away from the base station.

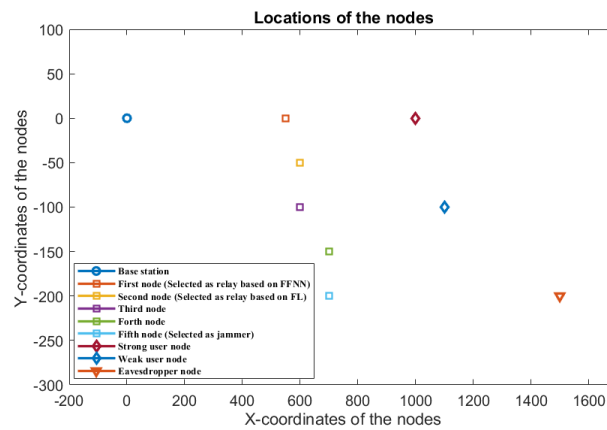


**Figure 7.** Locations of the nodes for the experiments

365 In this section, we evaluate the smart node selection by two experiments. Each experiment discusses  
 366 smart node selection based on FFNN and fuzzy logic strategies.

### 367 5.1. EXPERIMENT 1 (PROPOSED SMART NODE SELECTION BASED ON FFNN STRATEGY)

368 In this experiment, we propose a machine learning based on FFNN strategy to select the best cooperative  
 369 (relay, jammer) node. This strategy is proposed in order to enhance the physical layer security of the  
 370 cooperative NOMA system shown in Figure 1.

371 Table 5 illustrates the cooperative relay selection based on FFNN strategy. The relay selection criteria are  
 372 extracted based on the known CSI at the base-station.

**Table 5.** Cooperative relay selection based on feed forward neural networks

Node	Relay selection criteria			Relevance	Selection
	$SNR_{IJ}$	$PAF$	$D_{IJ}$		
1	0.8684	0.7213	0.7284	Very good	Selected
2	0.8522	0.6953	0.6429	Good	
3	0.4855	0.6844	0.5890	Medium	
4	0.3010	0.6920	0.5759	Medium	
5	0.1717	0.5429	0.6061	Bad	

373 Based on Table 5, we observe that the first cooperative node gives the best relay relevance (very good) in  
 374 comparison with the other cooperative nodes, hence it is selected by the base-station as the best cooperative  
 375 relay node. Table 6 illustrates the cooperative jammer selection based on FFNN strategy.

**Table 6.** Cooperative jammer selection based on feed forward neural networks

Node	Jammer selection criteria			Relevance	Selection
	$SNR_E$	$D_E$	$R_S$		
1	0.8981	0.6960	True	Very bad	
2	0.4372	0.6472	False	Bad	
3	0.2122	0.6037	False	Medium	
4	0.1197	0.5667	False	Medium	
5	0.0860	0.5375	False	Very good	Selected

376 In this paper, the priority is given to the relay selection. Hence, the first cooperative node is not selected  
 377 as the best jammer node. However, we observe that the fifth node provides the best jammer relevance

378 compared to the other cooperative nodes. Thus, it is selected as by the base-station the best cooperative  
379 jammer node.

## 380 5.2. EXPERIMENT 2 (SMART NODE SELECTION BASED ON FUZZY LOGIC SCHEME)

381 In this experiment, we use a smart node selection based on the fuzzy logic strategy to select the best  
382 cooperative (relay, jammer) node. Table 7 illustrates the cooperative relay selection based on fuzzy logic  
383 strategy. The relay selection criteria are the same as the criteria used in Table 5.

**Table 7.** Cooperative relay selection based on fuzzy logic selection scheme

Node	Relay selection criteria			Relevance	Selection
	$SNR_U$	$PAF$	$D_U$		
1	0.8684	0.7213	0.7284	Good	
2	0.8522	0.6953	0.6429	Good	Selected
3	0.4855	0.6844	0.5890	Medium	
4	0.3010	0.6920	0.5759	Bad	
5	0.1717	0.5429	0.6061	Very bad	

384 Based on Table 7, we observe that the first and second cooperative nodes give the best relay relevance  
385 (good) in comparison with the other cooperative nodes. However, fuzzy logic controller selects the second  
386 node as the best cooperative relay node. This is due to the distance significance compared to the first node.  
387 Table 8 illustrates the cooperative jammer selection based on the fuzzy logic strategy.

**Table 8.** Cooperative jammer selection based on fuzzy logic selection scheme

Node	Jammer selection criteria			Relevance	Selection
	$SNR_E$	$D_E$	$R_S$		
1	0.8981	0.6960	False	Bad	
2	0.4372	0.6472	True	Very bad	
3	0.2122	0.6037	False	Medium	
4	0.1197	0.5667	False	Good	
5	0.0860	0.5375	False	Very good	Selected

388 Based on Table 8, we observe that the fuzzy logic controller selects the same cooperative jammer node  
389 selected by the proposed FFNN strategy.

390 The outputs of these experiments are summarized as follows.

- 391 • The proposed FFNN strategy selects the first cooperative helper node as the relay node.
- 392 • The fuzzy logic scheme selects the second cooperative helper node as the relay node.
- 393 • Fifth cooperative helper node is selected as the jammer node by both approaches.

394 Figure 8 depicts the secrecy performance in terms of secrecy capacity within a range of total transmission  
395 power from 0 dBm to 30 dBm. The secrecy performance of the cooperative NOMA system is analysed for the  
396 proposed FFNN based node selection strategy and the fuzzy logic based node selection scheme.

397 Based on Figure 8, we observe that the secrecy capacity for each legal user is affected by several factors  
398 namely, the total transmission power, decoding abilities i.e., SIC, and strategy used for the cooperative node  
399 selection. Firstly, the secrecy capacity performance for each legal user is enhanced as the total transmission  
400 power and the shared-jamming power increased.

401 Based on Figure 8, we observe that the secrecy capacity of the strong user ( $\zeta_{u_1}$ ) is better than the secrecy  
402 performance of the weak user ( $\zeta_{u_2}$ ). The reason behind this is the successive interference cancellation  
403 technique used by the strong user. This technique enables the strong user to decode the information signal  
404 aimed to be sent to the weak user node. Thus, the strong user is not affected by the signal interference.



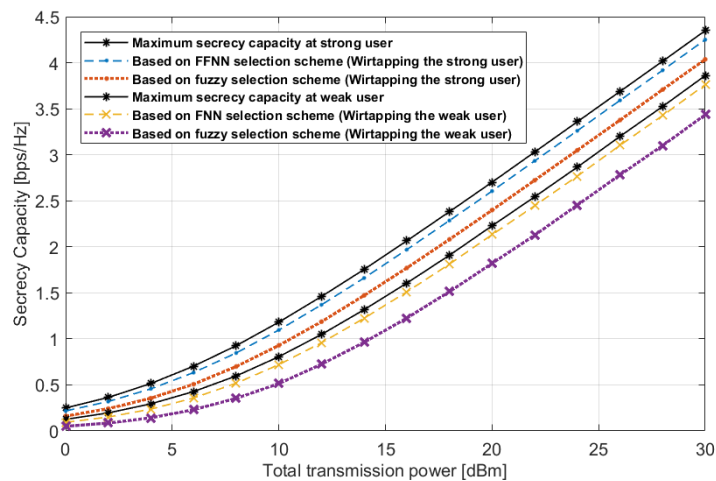


**Figure 8.** Secrecy capacity of the cooperative NOMA system assisted with smart node selection scheme

405 However, the weak user is affected by the strong user signal as the interference signal. Thus, the secrecy  
 406 capacity performance is decreased at the weak user.

407 Lastly, we observe that the proposed FFNN based node selection strategy provides high secrecy capacity  
 408 performance in comparison with the fuzzy logic scheme, This is due to the high estimation accuracy  
 409 established by the machine learning based on the feed forward neural network (FFNN) compared with  
 410 the fuzzy logic based selection scheme. The accuracy analysis of the cooperative node selection based on  
 411 FFNN strategy and fuzzy logic scheme is illustrated in Figure 9.

412 The accuracy analysis shown in Figure 9 is carried on by comparing the maximum secrecy capacity  
 413 performance of the cooperative NOMA system shown in Figure 1 (without considering the eavesdropper)  
 414 with the resulted secrecy capacity for the proposed node selection based on FFNN and the fuzzy logic based  
 415 node selection.

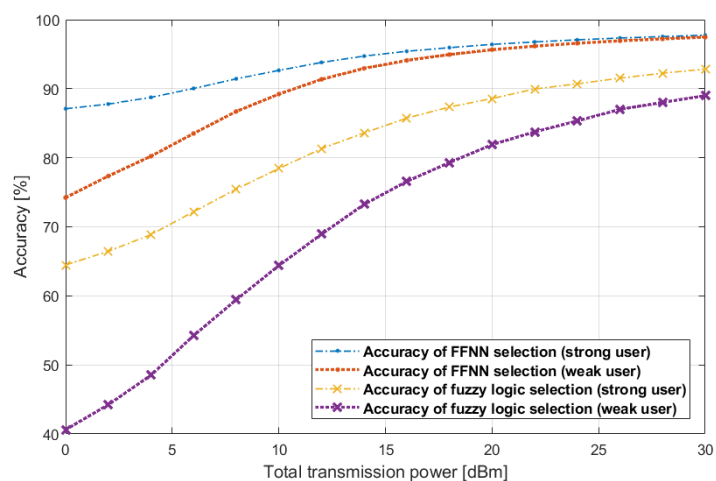


**Figure 9.** The cooperative node selection accuracy based on fuzzy logic and FFNN

416 Based on Figure 9, we observe that the accuracy of using the proposed strategy (FFNN based node  
 417 selection) in order to approach the maximum secrecy capacity (without eavesdropping) is higher than  
 418 accuracy of the fuzzy logic based scheme. In other words, the physical layer security of the cooperative  
 419 NOMA system model shown in Figure 1 using the proposed strategy is high in comparison with the fuzzy  
 420 logic scheme.

421 Table 9 illustrates the RMSe analysis for the smart node selection based on FFNN strategy and fuzzy  
422 logic scheme.

**Table 9.** Root mean square error (*RMSe*)

User nodes	Cooperative node selection strategy	
	Fuzzy logic	FFNN
Wiretapping strong user	0.2639	0.0846
Wiretapping weak user	0.3343	0.0859

423 Based on Table 9, we observe that the standard deviation (prediction errors) of the proposed strategy  
424 is lower than the fuzzy logic scheme for both legal user nodes. As summary of the comparison, the results  
425 obtained emphasizes that it is beneficial to use the proposed node selection based on FFNN strategy instead of  
426 the node selection based on fuzzy logic scheme.

## 427 6. Conclusion

428 In this paper, we proposed a strategy to enhance the physical layer security for a cooperative  
429 non-orthogonal multi access system. The proposed node selection strategy is integrated with a jamming  
430 null-steering beamforming technique in order to degrade the channel capacity of the eavesdropper node.  
431 Thus, enhancing the secrecy performance of the cooperative NOMA system. In conclusion, the results  
432 illustrate that the proposed cooperative node selection based on FFNN strategy outperforms the cooperative  
433 node selection based on fuzzy logic scheme due to the high estimation accuracy established by FFNN strategy.

434 For future work, we will consider the assumption of unknown CSI of the eavesdropper node  
435 at the base-station. Moreover, we will study the effect of relay protocols (detect-and-forward, and  
436 compress-and-forward) on the secrecy performance analysis. Furthermore, we will apply the proposed  
437 strategy on large cooperative NOMA scale where multi-eavesdropper nodes are considered.

## 438 Appendix A Trapezoidal function

439 In section 3 we mapped each parameter ( $SNR_U$ ,  $PAF$ ,  $D_U$ ,  $SNR_E$ ,  $D_E$  and  $R_S$ ) into a linguistic fuzzy  
440 sets functions. In order to describe these functions mathematically, we used the trapezoidal function. The  
441 trapezoidal function for the first parameter is given as [18],

$$\text{trapezoidal}(snr_u; v_1, c_1, c_2, v_2) = \begin{cases} \frac{x-v_1}{c_1-v_1}, & \text{if } snr_u \in [v_1, c_1] \\ 1, & \text{if } snr_u \in [c_1, c_2] \\ \frac{b-snr_u}{v_2-c_2}, & \text{if } snr_u \in [c_2, v_2] \\ 0, & \text{otherwise} \end{cases} \quad (A1)$$

442 where, ( $v_1, v_2$ ) are the valleys and ( $c_1, c_2$ ) are the climaxes of the trapezoidal function, such that  $v_1 <$   
443  $c_1 \leq c_2 < v_2$ . The particular case when  $c_1 = c_2$ , the function is not a trapezoidal function anymore, in fact it  
444 is a triangular function. In equation (A.1), the trapezoidal function maps the input parameter into a value  
445 between the interval [0,1] with degree of membership called  $\mu(sn r_u)$ . Similarly, the degree of membership  
446 of the other input parameters are  $\mu(sn r_u)$ ,  $\mu(paf)$ ,  $\mu(D_u)$ ,  $\mu(sn r_e)$ ,  $\mu(d_e)$  and  $\mu(r_s)$ ,  $\mu(Z_r)$ , and  $\mu(Z_j)$  are the  
447 degree of membership for the (relay, jammer) relevance parameters. We distributed the trapezoidal function  
448 for the first parameter ( $SNR_U$ ) as,

$$\begin{aligned} Low &= \text{trapezoidal}(snr_u; -0.4, 0, 0.2, 0.4), \\ Medium &= \text{trapezoidal}(snr_u; 0.2, 0.4, 0.6, 0.8), \\ High &= \text{trapezoidal}(snr_u; 0.7, 0.8, 1, 1.1). \end{aligned} \quad (A2)$$

449 Similarly, this relation can be rewritten for the other input and relevance parameters.

## 450 Appendix B Fuzzy logic block diagram for cooperative node selection

451 Figure 10 shows the block diagram of the fuzzy logic strategy used to select the best cooperative (relay,  
452 jammer) node.

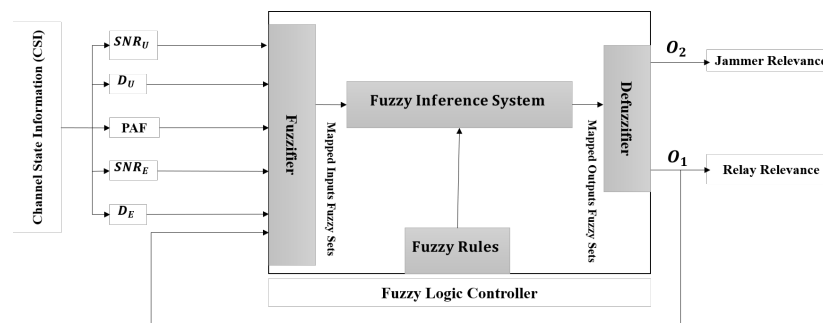


Figure A1. block diagram for cooperative node (relay, jammer) selection based on fuzzy logic

## 453 Acknowledgment

454 The supporter of this research is the TM Research and Development centre (TMRND).

## 455 References

456

- 457 1. M. A. Salem, A. B. Abd. Aziz, M. Y. Bin Alias and A. A. Abdul Rahman, "Secrecy Performance on Half-Duplex Two-Way  
458 Multi-Relay Transmission Technique Under Wireless Physical Layer Security," International Symposium on Information  
459 Theory and Its Applications (ISITA), Singapore, 2018, pp. 668-672.
- 460 2. C. E. Shannon, "Communication Theory of Secrecy Systems," in The Bell System Technical Journal, vol. 28, no. 4, pp.  
461 656-715, Oct. 1949.
- 462 3. A. D. Wyner, "The wire-tap channel," in The Bell System Technical Journal, vol. 54, no. 8, pp. 1355-1387, Oct. 1975.
- 463 4. T. M. Hoang, T. Q. Duong, H. A. Suraweera, C. Tellambura, and H. V. Poor, "Cooperative Beamforming and User  
464 Selection for Physical Layer Security in Relay Systems."
- 465 5. E. Nosrati, X. Wang, A. Khabbazibasmenj, and A. M. Akhtar, "Secrecy Enhancement Via Cooperative Relays in Multi-Hop  
466 Communication Systems," IEEE Veh. Technol. Conf., vol. 2016-July, no. iv, 2016.
- 467 6. A. Kumar and S. Sharma, "Secrecy Outage Probability with Destination Assisted Jamming in Presence of an Untrusted  
468 Relay," 2016.
- 469 7. A. Yener and S. Ulukus, "Wireless Physical-Layer Security: Lessons Learned from Information Theory," Proc. IEEE, vol.  
470 103, no. 10, pp. 1814-1825, 2015.
- 471 8. M. A. Salem, A. B. Abd. Aziz, M. Y. B. Alias, A. A. A. Rahman and A. Mahmud, "Secrecy Analysis on Half-Duplex Two-Way  
472 Relay Transmission Using Various Transmission Channels and Jamming Strategies," 7th International Conference on  
473 Computer and Communication Engineering (ICCCE), Kuala Lumpur, 2018, pp. 432-436.
- 474 9. M. A. Salem, A. AbdAziz, M. Y. Alias and A. A. A. Rahman, "Jamming Power Estimation Technique under Wireless  
475 Physical Layer Security in Presence of an Eavesdropper", accepted by the 7th International Conference on Smart  
476 Computing Communications, 2019, Malaysia.
- 477 10. Y. Zou, X. Wang and W. Shen, "Physical-Layer Security with Multiuser Scheduling in Cognitive Radio Networks," in  
478 IEEE Transactions on Communications, vol. 61, no. 12, pp. 5103-5113, December 2013.
- 479 11. M. Zhang and Y. Liu, "Energy Harvesting for Physical-Layer Security in OFDMA Networks," in IEEE Transactions on  
480 Information Forensics and Security, vol. 11, no. 1, pp. 154-162, Jan. 2016.
- 481 12. Z. Ding, X. Lei, G. K. Karagiannidis, R. Schober, J. Yuan and V. K. Bhargava, "A Survey on Non-Orthogonal Multiple  
482 Access for 5G Networks: Research Challenges and Future Trends," in IEEE Journal on Selected Areas in Communications,  
483 vol. 35, no. 10, pp. 2181-2195, Oct. 2017.
- 484 13. J. Chen, L. Yang and M. Alouini, "Physical Layer Security for Cooperative NOMA Systems," in IEEE Transactions on  
485 Vehicular Technology, vol. 67, no. 5, pp. 4645-4649, May 2018.

- 486 14. B. He, A. Liu, N. Yang and V. K. N. Lau, "On the Design of Secure Non-Orthogonal Multiple Access Systems," in IEEE  
487 Journal on Selected Areas in Communications, vol. 35, no. 10, pp. 2196-2206, Oct. 2017.
- 488 15. Y. Liu, Z. Qin, M. Elkashlan, Y. Gao and L. Hanzo, "Enhancing the Physical Layer Security of Non-Orthogonal Multiple  
489 Access in Large-Scale Networks," in IEEE Transactions on Wireless Communications, vol. 16, no. 3, pp. 1656-1672,  
490 March 2017.
- 491 16. K. Sasaki, X. Liao and X. Jiang, "Cooperative Jamming in a Two-Hop Relay Wireless Network with Buffer-Aided Relays,"  
492 2017 Fifth International Symposium on Computing and Networking (CANDAR), Aomori, 2017, pp. 565-569.
- 493 17. G. Brante, G. de Santi Peron, R. D. Souza and T. Abrão, "Distributed Fuzzy Logic-Based Relay Selection Algorithm for  
494 Cooperative Wireless Sensor Networks," in IEEE Sensors Journal, vol. 13, no. 11, pp. 4375-4386, Nov. 2013.
- 495 18. B. Razeghi, M. Hatamian, A. Naghizadeh, S. Sabeti and G. A. Hodtani, "A Novel Relay Selection Scheme For Multi-User  
496 Cooperation Communications Using Fuzzy Logic," 2015 IEEE 12th International Conference on Networking, Sensing  
497 and Control, Taipei, 2015, pp. 241-246.
- 498 19. N. Taj, M. H. Zafar, S. A. Waqas, H. Rehman, M. O. Alassafi and I. Khan, "Smart Relay Selection Scheme Based on Fuzzy  
499 Logic with Optimal Power Allocation and Adaptive Data Rate Assignment" International Journal of Communication  
500 Networks and Information Security (IJCNIS), vol. 11, no. 1, pp. 239-247, April 2019.
- 501 20. J. Ahmad, H. Larijani, R. Emmanuel, M. Mannion and A. Qureshi, "Secure Occupancy Monitoring System for IoT Using  
502 Lightweight Intertwining Logistic Map," 2018 10th Computer Science and Electronic Engineering (CEECE), Colchester,  
503 United Kingdom, 2018, pp. 208-213.
- 504 21. L. Lei, T. X. Vu, L. You, S. Fowler and D. Yuan, "Efficient Minimum-Energy Scheduling with Machine-Learning Based  
505 Predictions for Multiuser MISO Systems," 2018 IEEE International Conference on Communications (ICC), Kansas City,  
506 MO, 2018, pp. 1-6.
- 507 22. Y. Sun, M. Peng, Y. Zhou, Y. Huang and S. Mao, "Application of Machine Learning in Wireless Networks: Key Techniques  
508 and Open Issues," in IEEE Communications Surveys and Tutorials.
- 509 23. T. T. Nguyen, J. H. Lee, M. T. Nguyen, Y. H. Kim, "Machine Learning-Based Relay Selection for Secure Transmission in  
510 Multi-Hop DF Relay Networks" Multidisciplinary Digital Publishing Institute (MDPI) on Electronics, vol. 11, no. 1, pp.  
511 239-247, August 2019.
- 512 24. D. He, C. Liu, T. Q. S. Quek and H. Wang, "Transmit Antenna Selection in MIMO Wiretap Channels: A Machine  
513 Learning Approach," in IEEE Wireless Communications Letters, vol. 7, no. 4, pp. 634-637, Aug. 2018.
- 514 25. C. Wen, S. Jin, K. Wong, J. Chen and P. Ting, "Channel Estimation for Massive MIMO Using Gaussian-Mixture Bayesian  
515 Learning," in IEEE Transactions on Wireless Communications, vol. 14, no. 3, pp. 1356-1368, March 2015.
- 516 26. R. Amiri, H. Mehrpouyan, L. Fridman, R. K. Mallik, A. Nallanathan and D. Matolak, "A Machine Learning Approach for  
517 Power Allocation in HetNets Considering QoS," 2018 IEEE International Conference on Communications (ICC), Kansas  
518 City, MO, 2018, pp. 1-7.
- 519 27. J. Joung, "Machine Learning-Based Antenna Selection in Wireless Communications," in IEEE Communications  
520 Letters, vol. 20, no. 11, pp. 2241-2244, Nov. 2016.
- 521 28. Y. Zhang, H. Wang, Q. Yang and Z. Ding, "Secrecy Sum Rate Maximization in Non-orthogonal Multiple Access," in  
522 IEEE Communications Letters, vol. 20, no. 5, pp. 930-933, May 2016.
- 523 29. H. Deng, H. Wang, W. Guo and W. Wang, "Secrecy Transmission With a Helper: To Relay or to Jam," in IEEE Transactions  
524 on Information Forensics and Security, vol. 10, no. 2, pp. 293-307, Feb. 2015.
- 525 30. T. M. Hoang, T. Q. Duong, H. A. Suraweera, C. Tellambura and H. V. Poor, "Cooperative Beamforming and User  
526 Selection for Improving the Security of Relay-Aided Systems," in IEEE Transactions on Communications, vol. 63, no. 12,  
527 pp. 5039-5051, Dec. 2015.
- 528 31. Z. Mobini, M. Mohammadi and C. Tellambura, "Wireless-Powered Full-Duplex Relay and Friendly Jamming for Secure  
529 Cooperative Communications," in IEEE Transactions on Information Forensics and Security, vol. 14, no. 3, pp. 621-634,  
530 March 2019.
- 531 32. Y. Alsaba, C. Y. Leow and S. K. Abdul Rahim, "A Game-Theoretical Modelling Approach for Enhancing the Physical  
532 Layer Security of Non-Orthogonal Multiple Access System," in IEEE Access, vol. 7, pp. 5896-5904, 2019.
- 533 33. J. Chen, L. Yang and M. Alouini, "Physical Layer Security for Cooperative NOMA Systems," in IEEE Transactions on  
534 Vehicular Technology, vol. 67, no. 5, pp. 4645-4649, May 2018.
- 535 34. G. Chen and T. T. Pham, Introduction to Fuzzy Sets, Fuzzy Logic, and Fuzzy Control Systems. CRC press, 2001.